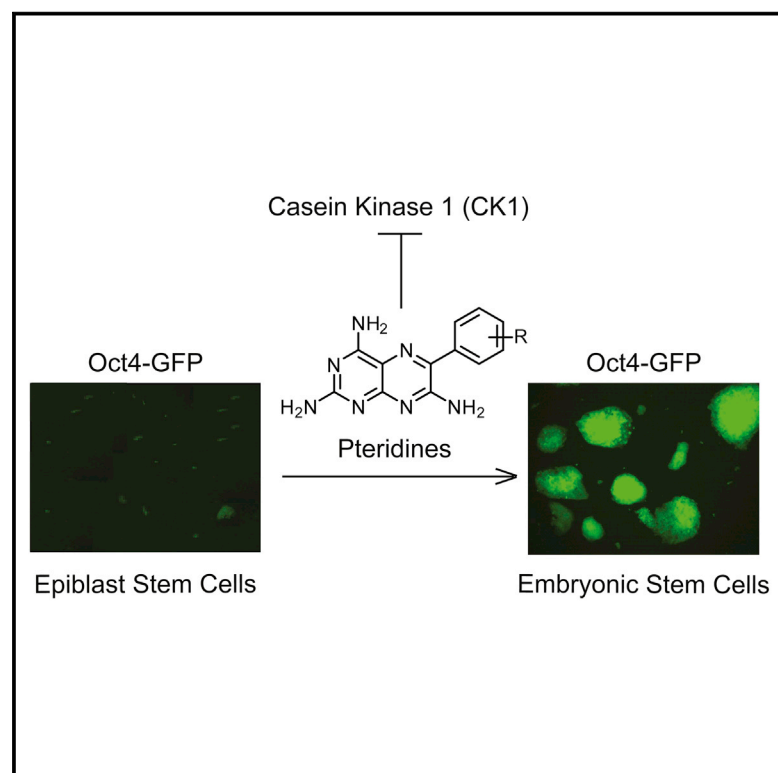


Cell Chemical Biology

Epiblastin A Induces Reprogramming of Epiblast Stem Cells Into Embryonic Stem Cells by Inhibition of Casein Kinase 1

Graphical Abstract



Authors

Andrei Ursu, Damir J. Illich,
Yasushi Takemoto, ..., Slava Ziegler,
Hans R. Schöler, Herbert Waldmann

Correspondence

office@mpi-muenster.mpg.de (H.R.S.),
herbert.waldmann@mpi-dortmund.mpg.
de (H.W.)

In Brief

Ursu et al. identified Epiblastin A, which efficiently converts epiblast stem cells into embryonic stem cells by inhibition of casein kinase 1.

Highlights

- Triamterene induces reprogramming of epiblast stem cells
- Triamterene targets casein kinases 1 (CK1) for stem cell reprogramming
- Structure-based compound development yielded the novel CK1 inhibitor Epiblastin A
- Epiblastin A displays high reprogramming activity

Accession Numbers

5IH4
5IH5
5IH6



Epiblastin A Induces Reprogramming of Epiblast Stem Cells Into Embryonic Stem Cells by Inhibition of Casein Kinase 1

Andrei Ursu,^{1,2,8} Damir J. Illich,^{3,8} Yasushi Takemoto,^{4,9} Arthur T. Porfetye,^{2,5} Miao Zhang,³ Andreas Brockmeyer,¹ Petra Janning,¹ Nobumoto Watanabe,^{4,6} Hiroyuki Osada,^{4,6} Ingrid R. Vetter,⁵ Slava Ziegler,¹ Hans R. Schöler,^{3,7,*} and Herbert Waldmann^{1,2,*}

¹Department of Chemical Biology, Max Planck Institute of Molecular Physiology, Otto-Hahn-Strasse 11, 44227 Dortmund, Germany

²Chemical Biology, Faculty of Chemistry and Chemical Biology, Technical University Dortmund, Otto-Hahn-Strasse 6, 44221 Dortmund, Germany

³Department of Cell and Developmental Biology, Max Planck Institute for Molecular Biomedicine, Röntgenstrasse 20, 48149 Münster, Germany

⁴Bioprobe Research Group, RIKEN-Max Planck Joint Research Center for Systems Chemical Biology, RIKEN Global Research Cluster, 2-1 Hirosawa, Wako, Saitama 351-0198, Japan

⁵Department of Mechanistic Cell Biology, Max Planck Institute of Molecular Physiology, Otto-Hahn-Strasse 11, 44227 Dortmund, Germany

⁶Chemical Biology Research Group, RIKEN Center for Sustainable Resource Science, 2-1 Hirosawa, Wako, Saitama 351-0198, Japan

⁷University of Münster, 48149 Münster, Germany

⁸Co-first author

⁹Present address: Institute for Chemical Research, Kyoto University, Uji, Kyoto 611-0011, Japan

*Correspondence: office@mpi-muenster.mpg.de (H.R.S.), herbert.waldmann@mpi-dortmund.mpg.de (H.W.)

<http://dx.doi.org/10.1016/j.chembiol.2016.02.015>

SUMMARY

The discovery of novel small molecules that induce stem cell reprogramming and give efficient access to pluripotent stem cells is of major importance for potential therapeutic applications and may reveal novel insights into the factors controlling pluripotency. Chemical reprogramming of mouse epiblast stem cells (EpiSCs) into cells corresponding to embryonic stem cells (cESCs) is an inefficient process. In order to identify small molecules that promote this cellular transition, we analyzed the LOPAC library in a phenotypic screen monitoring Oct4-GFP expression and identified tramterene (TR) as initial hit. Synthesis of a TR-derived compound collection and investigation for reprogramming of EpiSCs into cESCs identified casein kinases 1 (CK1) $\alpha/\delta/\epsilon$ as responsible cellular targets of TR and unraveled the structural parameters that determine reprogramming. Delineation of a structure-activity relationship led to the development of Epiblastin A, which engages CK1 isoenzymes in cell lysate and induces efficient conversion of EpiSCs into cESCs.

INTRODUCTION

Stem cell research and technology have recently emerged as powerful approaches to the development of cell-based therapies for various diseases (Wei et al., 2013; Volarevic et al., 2014; Lunn et al., 2014), tissue engineering (Forbes and Rosenthal, 2014), and disease modeling (Grskovic et al., 2011; Sternecker et al.,

2014). In particular the identification of methods giving access to pluripotent stem cells (PSCs) that can self-renew and differentiate into all somatic cell types is of major importance (González et al., 2011; Kejin, 2014). The establishment of such methods in turn could potentially reveal novel insights into the factors governing stem cell self-renewal and differentiation, as well as de- and transdifferentiation (Boiani and Scholer, 2005; Ng and Surani, 2011; Shenghui et al., 2009).

In the context of cell reprogramming, the identification of small molecules that can regulate stem cell fate and replace crucial elements of the transcription factor network controlling pluripotency has gained substantial attention (Shi et al., 2008; Huangfu et al., 2008; Federation et al., 2014). For instance, recently the reprogramming of differentiated cells into PSCs could be achieved by chemical means only, using a cocktail of seven small molecules (Hou et al., 2013). Initially, reprogramming to induced pluripotent stem cells (iPSCs) was accomplished by expressing the transcription factors Oct4, Sox2, Klf4, and c-Myc in mouse fibroblasts (Takahashi and Yamanaka, 2006).

So far, two types of PSCs have been derived from early mammalian embryos, termed embryonic stem cells (ESCs) and epiblast stem cells (EpiSCs). Like iPSCs, mouse ESCs are in a state of naive pluripotency (Nichols and Smith, 2009), whereas mouse EpiSCs (Brons et al., 2007; Tesar et al., 2007) feature primed pluripotency (Nichols and Smith, 2009). Primed EpiSCs can be converted into cells corresponding to naive ESCs, which we term cESCs to distinguish them from blastocyst-derived ESCs. Naive pluripotency is induced in EpiSCs when they are exposed to ESC culture conditions supplemented with a cocktail referred to as 2i/LIF, which is composed of MEK1 inhibitor PD0325901, GSK-3 β inhibitor CHIR-99021, and leukemia inhibitory factor (LIF) (Hanna et al., 2009; Greber et al., 2010). However, we have shown that the EpiSC line derived from GOF18 (genomic Oct4 fragment, 18 kb) mice, containing a

GFP transgene under the control of the entire regulatory region of the *Oct4* gene (Yeom et al., 1996), is heterogeneous (Han et al., 2010). These cells consist of two distinct populations that differ in the expression levels of specific fluorescently tagged *Oct4* (Han et al., 2010), a crucial pluripotency-associated transcription factor (Jerabek et al., 2014; Radzishewska and Silva, 2014). We found that exposure to 2i/LIF converted only a minor, *Oct4*-GFP-positive fraction of EpiSCs (less than 1% of the entire cell population) into cESCs, whereas the *Oct4*-GFP negative cells (more than 99% of the entire cell population) were not. In order to efficiently reprogram more EpiSCs we searched for a small-molecule modulator that would efficiently restore the *Oct4*-GFP expression in EpiSCs and potentially convert them to naive cESCs. Identification of the corresponding target proteins and the pathways responsible for the reprogramming activity would give deeper insights into the mechanisms that regulate stem cell dedifferentiation and pave the way for the development of more efficient protocols to obtain naive cESCs. Here we report on the development of a high-content screening platform that monitors the efficient reactivation of *Oct4*-GFP expression in EpiSCs. Evaluation of the LOPAC library in the reprogramming assay yielded a single hit, triamterene (TR). The subsequent synthesis of a small compound collection yielded compounds with increased reprogramming activity compared with TR. These compounds were collectively termed Epiblastins. We show that the Epiblastins inhibit casein kinase 1 (CK1) α , δ , and ϵ to various extents. The most active compound was named Epiblastin A and engages CK1 $\alpha/\delta/\epsilon$ isoforms in lysates derived from the human colorectal carcinoma HCT116 cell line. Genetic ablation of CK1 α and to a lower extent CK1 ϵ by means of RNAi reproduced the dedifferentiation phenotype indicating that inhibition of this kinase family is important at later stages of the reprogramming process in mouse stem cells.

RESULTS

TR Induces the Reactivation of *Oct4*-GFP Expression in EpiSCs

An *Oct4* reporter line termed GOF18, which harbors all known *Oct4* regulatory elements, was used to study the different states of pluripotency (Yeom et al., 1996). Previous reports showed that E3 GOF18-ESCs express GFP when cultured under ESC conditions (Han et al., 2010; Bernemann et al., 2011). The corresponding E3 GOF18-EpiSCs, when cultured under EpiSC conditions (i.e., basic fibroblast growth factor [bFGF] and Activin A) do not express GFP, except for a small subpopulation of less than 1% (Han et al., 2010). The E3 *Oct4*-GFP-negative GOF18 EpiSCs (more than 99% of the entire cell population) were found to be refractive to 2i/LIF-based ESC conversion, thus dramatically limiting the access to cESCs. Based on these findings, we set out to identify small molecules that are capable of restoring efficient *Oct4*-GFP expression in E3 GOF18-EpiSCs (see [Supplemental Information](#) for more details). For this purpose, we developed a high-content imaging screening platform in 96-well format (see [Figure 1A](#)). The quantitative readout was based on the number of cells with GFP intensity above a preset minimum value, with a threshold set according to the levels of ESCs (see [Figure 1B](#)). Moreover, the assay can also monitor the morphological changes, which represent important criteria to assess

the extent of the reprogramming process. For example, EpiSCs form large and flat colonies, whereas ESCs grow as a small and compact 3D cell population (see [Figure 1A](#)). 2i/LIF ESC medium was used as a positive control and conditioned medium/fibroblast growth factor (CM/FGF) EpiSC medium was employed as a negative control (see [Figure S1](#)). The quality of the assay was validated using the Z' factor, which was calculated to be 0.57 (Zhang et al., 1999). We then screened the Library of Pharmacologically Active Compounds (LOPAC), which contains annotated agents with known target proteins, and therefore should enable rapid target hypothesis generation. The screening campaign yielded a single active compound that was capable of inducing a significant increase in the number of *Oct4*-GFP-positive cells in the E3 GOF18-EpiSC population (see [Figure 1C](#)). The hit TR (see chemical structure in [Figure 1D](#)) is a pteridine-based compound that blocks the epithelial sodium channel (ENaC) (Kellenberger et al., 2003) and is used as a diuretic in the clinic (Busch et al., 1996). The conversion occurred despite the presence of bFGF and Activin A in the growth medium, which promote the maintenance of EpiSCs in culture. This suggests that the mode of action of TR requires the signaling pathways responsible for the self-renewal of this cell population. A close inspection of the cellular morphology showed that the reprogrammed cells acquired a compact 3D morphology characteristic for ESCs. This observation indicates that the *Oct4*-GFP expressing cell population reached an ESC-like state. Taken together, we identified a small molecule that turns on the *Oct4*-GFP transgene expression in E3 GOF18-EpiSC cells and, therefore, can be regarded as a reprogramming inducer of mouse EpiSCs.

TR Induces *Oct4*-GFP Expression by Inhibiting CK1

Since TR is an antagonist of the ENaC channel (Kellenberger et al., 2003), we investigated whether this mode of action was responsible for the observed reprogramming activity. However, functional investigation of the structurally unrelated ENaC antagonist amiloride revealed that this activity of TR is not decisive for reprogramming EpiSCs (see [Figure 2A](#)). Since the closely related TR derivative, TG100-115 (Palanki et al., 2007), has previously been described as an inhibitor of the phosphatidylinositol 3-kinases (PI3K) (Davis et al., 2011; Doukas et al., 2006), we investigated whether this protein family might be targeted by TR and performed a focused kinase profiling study including various members of the lipid kinase family (see [Table S1](#)). TR blocked the enzymatic activity of different PI3Ks (see [Table S1](#)). Therefore, we investigated whether inhibition of PI3Ks by TR might be responsible for the reprogramming process and analyzed the structurally unrelated PI3K inhibitors AS-605240 and LY294002. These inhibitors did not turn on the expression of the *Oct4*-GFP transgene in EpiSCs (see [Figure 2A](#)), suggesting that pharmacological inhibition of PI3K is not responsible for the reprogramming activity. Given the facts that TR is not an optimized, selective kinase inhibitor and that kinases share high structure and sequence homology in their ATP-binding sites, we hypothesized that TR might target a different kinase to induce the reactivation of the *Oct4*-GFP expression in EpiSCs. We subjected TR to an additional extended kinase profiling study that included 119 kinases, comprising members of the most important signaling pathways found to modulate stem cell fate in processes such as reprogramming and differentiation (see [Table](#)

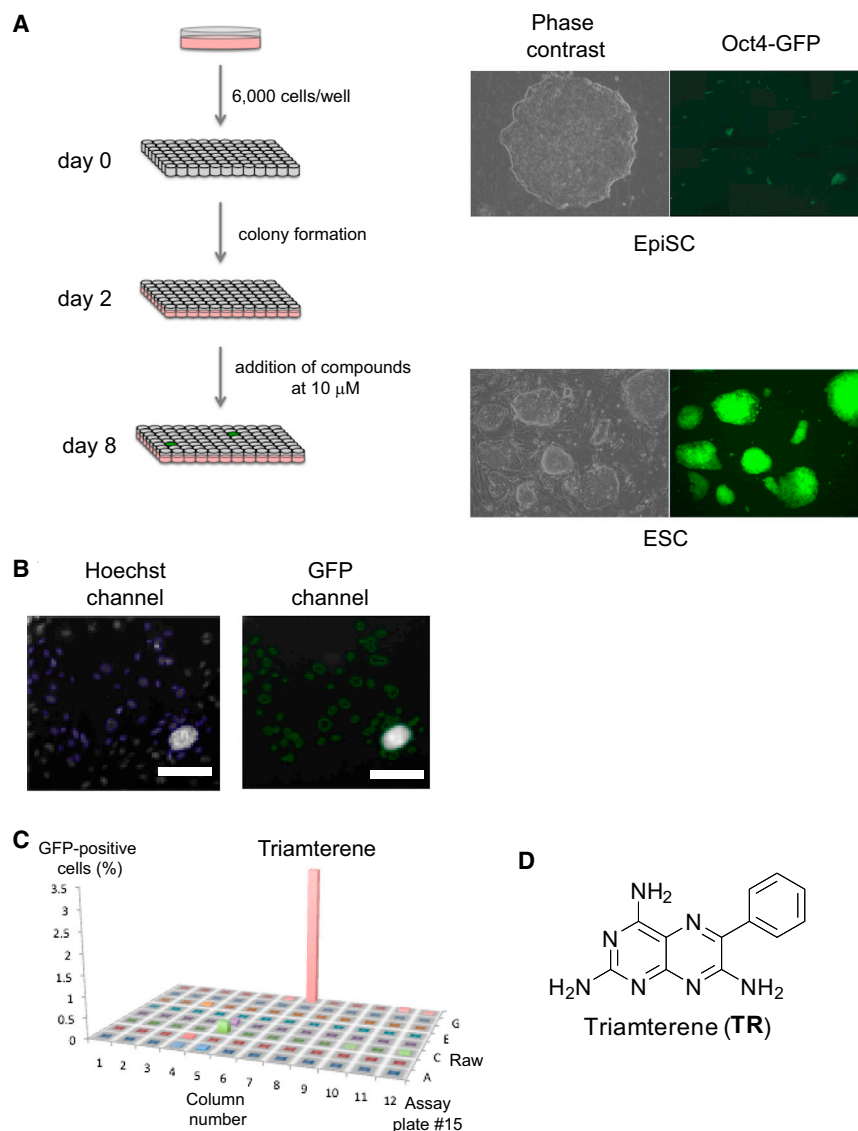


Figure 1. Stem Cell-Based Screening Assay Identifies Triamterene as an Inducer of Epiblast Stem Cell Reprogramming

(A) Schematic representation of the small-molecule screening assay based on the reactivation of Oct4-GFP in E3 GOF18-EpiSCs. EpiSCs were seeded as single cells on FCS-coated 96-well plates in EpiSC culture medium (CM/FGF) on day 0. Compounds were added on day 2 at 10 μ M concentration in EpiSC CM without additional FGF. EpiSC culture medium was used as a negative control, and ESC medium including 2i/LIF was used as a positive control. The cell colonies were dissociated into single cells using trypsin on day 8, and GFP-positive cells were quantified by means of the high-content reader ArrayScan.

(B) Readout system based on consequent fluorescence imaging for Hoechst nuclei stain and Oct4-GFP with ArrayScan. Scale bar represents 200 μ m.

(C) Identification of the hit compound triamterene located in rack number 15, position H07 of the LOPAC library. GFP-positive cells (%), percentage of cells with GFP signal above the preset threshold.

(D) Chemical structure of the hit compound triamterene (TR).

See also Figure S1.

ously known ENaC blocker, targets members of the PI3K and CK1 kinase family. Moreover, we revealed that only the inhibition of CK1 generated Oct4-GFP colonies within the EpiSC population, thereby connecting this kinase family to the induction of the later stages of reprogramming in mouse stem cells.

Synthesis of a Compound Collection and Delineation of a Structure-Activity Relationship

Having identified TR as an Oct4-inducing agent in EpiSCs, we set out to confirm the reprogramming activity associated

S2). In addition to PI3K isoforms, TR was identified as a fairly selective inhibitor of CK1 α , δ , and ϵ isoenzymes, but not affecting CK1 γ 1, γ 2, γ 3, and CK2 (see Figure 2B). Indeed, concentration dependent analyses showed half maximal inhibitory concentration (IC₅₀) values of 33.5 μ M, 6.9 μ M, and 30.4 μ M for CK1 α , CK1 δ , and CK1 ϵ isoenzymes, respectively (see Figure 2C). To validate the involvement of the CK1 family in the reactivation of Oct4-GFP expression in EpiSCs, we tested a structurally unrelated pan-CK1 inhibitor D4476 (Rena et al., 2004). GFP-positive colonies could be detected under the same assay conditions although to a lower extent than observed upon treatment with TR, confirming the involvement of the CK1 isoenzymes in reprogramming EpiSCs (see Figure 2D). We attribute the lower conversion efficiency of D4476 to the inhibition of undesired protein kinases (off-targets), which is common for even highly selective and optimized kinase inhibitors. This activity might negatively interfere with the signaling pathways responsible for reprogramming, and thus might explain the observed discrepancy in the biological activity. Taken together, we showed that TR, a previ-

ously known ENaC blocker, targets members of the PI3K and CK1 kinase family. Moreover, we revealed that only the inhibition of CK1 generated Oct4-GFP colonies within the EpiSC population, thereby connecting this kinase family to the induction of the later stages of reprogramming in mouse stem cells.

with the pteridine scaffold by generating closely related analogs that might yield more active derivatives. Using either commercially available or readily accessible starting materials (see derivatives 1–4, Figures 3A and 3B), we generated 36 compounds in order to explore the correlation between structure and biological activity. Thus, initially we varied the substitution pattern on the benzene ring following known synthesis procedures (Spickett and Timmis, 1954; Weinstock et al., 1968; Osdene et al., 1967). To this end, commercially available 5-nitroso-2,4,6-triaminopyrimidine 1 was reacted with a broad range of phenylacetoneitriles to yield in a single step derivatives 5–33 decorated with various substituents on position C6 of the pteridine core (see Figure 3A). In addition, derivatives 34–36 carrying various groups in positions C6 and C7 of the pteridine scaffold were synthesized from starting compound 4 (Palanki et al., 2007) (see Figure 3B). Compounds 37–40, which contain various substitutions at the C2 amino group were generated starting from nitroso-derivatives 2 and 3 (Spickett and Timmis, 1954) (see Figure 3A). Investigation of the resulting 36 compounds for reprogramming of

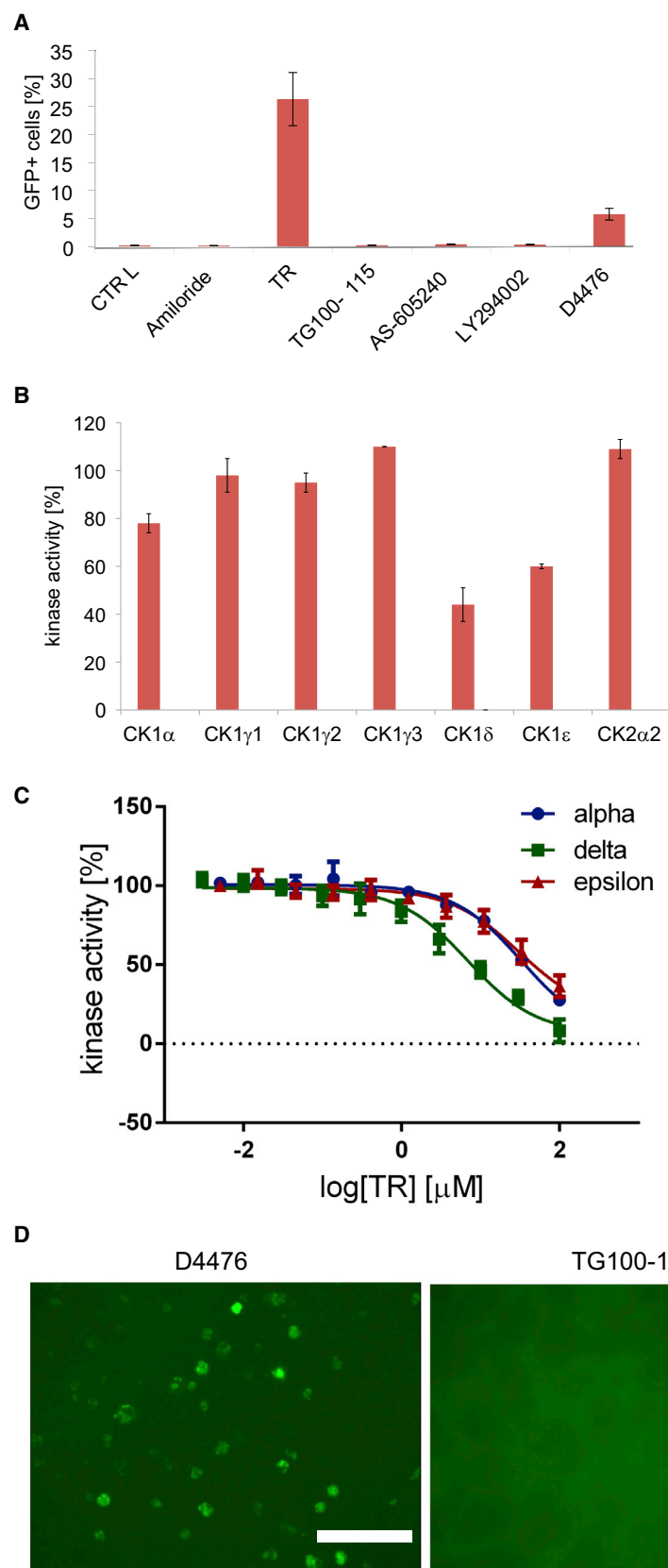


Figure 2. Triamterene Induces Oct4-GFP Expression in EpiSCs by Targeting the Casein Kinase 1 Family

(A) Influence of ENaC inhibitor amiloride (10 μ M), PI3K inhibitors TG100-115 (10 μ M), AS605240 (10 μ M), and LY294002 (10 μ M), and CK1 inhibitor D4476 (20 μ M) on the induction of Oct4-GFP expression in E3 GOF18-EpiSCs as determined by flow cytometry. Data represent mean values \pm SEM of three independent measurements.

(B) Focused kinase profiling study using a radio-metric readout for the inhibition of casein kinase isoenzymes upon treatment with 10 μ M triamterene (TR). Data represent mean values \pm SEM of three independent measurements.

(C) Dose-response curves for inhibition of CK1 α (IC_{50} = 33.5 μ M), CK1 δ (IC_{50} = 6.9 μ M), and CK1 ϵ (IC_{50} = 30.4 μ M) upon treatment with triamterene (TR). Data represent mean values \pm SEM of three independent measurements. Determined IC_{50} value \pm SEM was generated by fitting the data with three-parameter nonlinear regression analysis.

(D) Oct4-GFP expression in E3 GOF18-EpiSCs after 6 days treatment with the CK1 inhibitor D4476 (20 μ M) and the PI3K inhibitor TG100-115 (10 μ M). Scale bar, 300 μ m. Data are representative of three independent experiments.

See also Table S1 and Table S2.

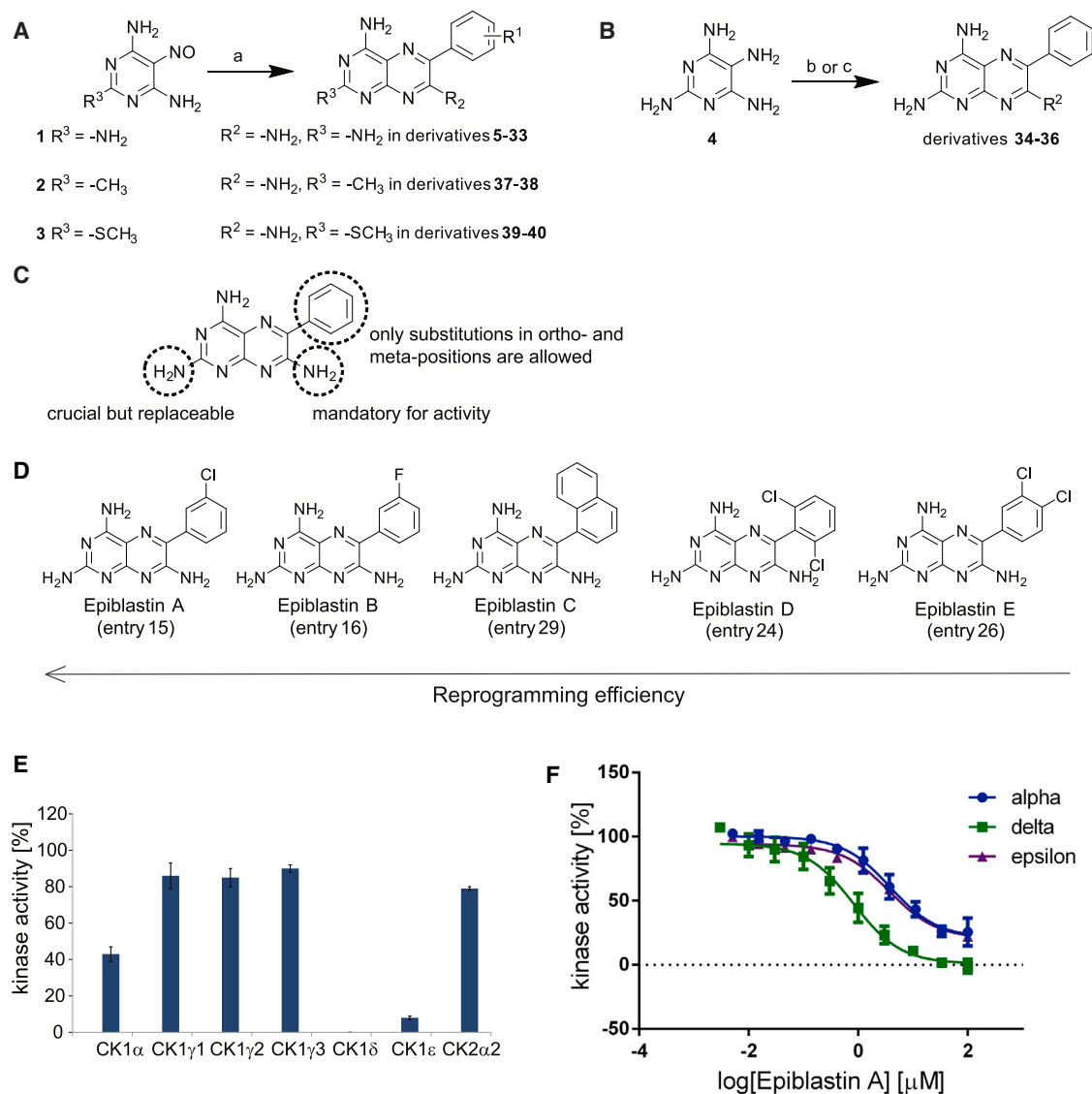


Figure 3. Epiblastin A Shows Increased Reprogramming Activity

(A) Synthesis of pteridine derivatives bearing substitutions at positions C2 and C6. Reaction condition a, phenylacetonitrile (1.1 eq), NaH (1.1 eq), 2-ethoxyethanol, reflux (1–3 hr).

(B) Synthesis of pteridine compounds containing various substitutions at position C7. Reaction condition b, NaHCO₃ (2 eq), H₂O, then benzil (1 eq), reflux (3 hr); reaction condition c, phenylglyoxal (1.1 eq), hydroxylamine hydrochloride (1.1 eq), MeOH, reflux.

(C) Structure-activity relationship study derived from the capacity to induce reprogramming of EpiSCs.

(D) Chemical structures of Epiblastins A–E. Numbers contained in brackets indicate the entry number of these compounds in Table 1.

(E) Focused kinase profiling inhibition study using radiometric readout of casein kinase isoenzymes upon treatment with 10 μ M Epiblastin A. Data represent mean values \pm SEM of three independent measurements.

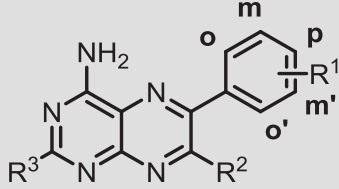
(F) Dose-response curves for inhibition of CK1 α (IC₅₀ = 3.8 μ M), CK1 δ (IC₅₀ = 0.8 μ M), and CK1 ϵ (IC₅₀ = 3.7 μ M) upon treatment with Epiblastin A. Data represent mean values \pm SEM of three independent measurements. Determined IC₅₀ value \pm SEM was generated by fitting the data with three-parameter nonlinear regression analysis.

See also Table S3.

EpiSCs (entries **5–40**, Table 1) revealed that even small alterations of the phenyl ring at C6 of the pteridine scaffold substantially affected the conversion efficiency (entries **5–33**, Table 1). For example, introduction of a fluorine atom in the *para*-position reduced the relative reprogramming efficiency by 40% (entry **6**; the reprogramming activity for TR, entry **5**, was arbitrarily set to

1). Introduction of larger *para*-substituents such as methoxy in compound **8** (entry **8**), methyl in compound **9** (entry **9**), or amino in compound **10** (entry **10**) led to a larger reduction or complete loss of activity. Thus, the *para*-position of the phenyl ring must remain unsubstituted to maintain the reprogramming activity. However, variation of the substituents in the *meta*-position was

Table 1. Reprogramming Efficiencies of EpiSCs and CK1 $\alpha/\delta/\epsilon$ Inhibiting Activity upon Treatment with Pteridine Derivatives 5–40

							
No.	R ¹	R ²	R ³	Efficiency	CK1 α IC ₅₀ (μM)	CK1 δ IC ₅₀ (μM)	CK1 ϵ IC ₅₀ (μM)
5	-H	-NH ₂	-NH ₂	1	36.8 ± 5.6	36.4 ± 6.4	26.8 ± 4.2
6	p-F	-NH ₂	-NH ₂	0.6	NT	ND	ND
7	p-OAllyl	-NH ₂	-NH ₂	0.1	NT	ND	ND
8	p-OCH ₃	-NH ₂	-NH ₂	0.1	NT	ND	ND
9	p-CH ₃	-NH ₂	-NH ₂	0.07	NT	ND	ND
10	p-NH ₂	-NH ₂	-NH ₂	0	NT	81.2 ± 15.8	ND
11	p-NO ₂	-NH ₂	-NH ₂	0	NT	ND	ND
12	p-iPr	-NH ₂	-NH ₂	0	NT	ND	ND
13	p-Ph	-NH ₂	-NH ₂	0	NT	ND	ND
14	p-OBz	-NH ₂	-NH ₂	0	NT	ND	ND
15	m-Cl	-NH ₂	-NH ₂	8.4	8.9 ± 2.4	0.5 ± 0.1	4.7 ± 0.8
16	m-F	-NH ₂	-NH ₂	3.1	33.3 ± 5.9	61.8 ± 12.5	14.4 ± 4.7
17	m-Me	-NH ₂	-NH ₂	1.6	NT	20.2 ± 4.7	ND
18	m-Br	-NH ₂	-NH ₂	1.1	9.3 ± 1.9	2.5 ± 0.5	ND
19	m-CF ₃	-NH ₂	-NH ₂	0.7	NT	ND	ND
20	m-OCH ₃	-NH ₂	-NH ₂	0.3	NT	12.3 ± 1.9	26.3 ± 4.9
21	m-NH ₂	-NH ₂	-NH ₂	0.2	NT	32.4 ± 7.0	12.4 ± 3.0
22	o-OCH ₃	-NH ₂	-NH ₂	1.3	NT	ND	ND
23	o-F	-NH ₂	-NH ₂	1.3	NT	ND	28.3 ± 3.8
24	o,o'-diCl	-NH ₂	-NH ₂	2.2	NT	ND	38.9 ± 5.8
25	o,p-diCl	-NH ₂	-NH ₂	0.5	55.6 ± 8.2	ND	4.3 ± 0.9
26	m,p-diCl	-NH ₂	-NH ₂	1.6	NT	ND	ND
27	o,o'-diF	-NH ₂	-NH ₂	2.3	NT	35.7 ± 5.2	51.5 ± 11.8
28	m,o'-diF	-NH ₂	-NH ₂	0.8	NT	ND	38.4 ± 6.1
29	naphthalen-1-yl	-NH ₂	-NH ₂	2.6	35.9 ± 6.6	36.5 ± 6.4	1.0 ± 0.2
30	pyridin-2-yl	-NH ₂	-NH ₂	0.5	ND	ND	6.6 ± 1.9
31	benzo[b]thiophen-3-yl	-NH ₂	-NH ₂	0.4	5.6 ± 1.1	2.8 ± 0.4	0.6 ± 0.1
32	thiophen-2-yl	-NH ₂	-NH ₂	0.1	14.2 ± 3.0	24.4 ± 6.4	8.1 ± 2.5
33	pyridin-3-yl	-NH ₂	-NH ₂	0.01	NT	16.1 ± 4.3	15.5 ± 4.0
34	-Ph	-Ph	-NH ₂	0.5	NT	ND	ND
35	-Ph	-H	-NH ₂	0.1	29.5 ± 5.0	80.6 ± 11.7	6.0 ± 1.5
36	m-OH-Ph	m-OH-Ph	-NH ₂	0.07	5.5 ± 1.3	9.6 ± 1.6	6.6 ± 1.5
37	m-H	-NH ₂	-CH ₃	0	NT	ND	ND
38	m-F	-NH ₂	-CH ₃	0	NT	ND	ND
39	m-H	-NH ₂	-SCH ₃	0.08	NT	ND	ND
40	m-F	-NH ₂	-SCH ₃	1.72	NT	ND	ND

The relative reprogramming activity of triamterene (**TR**, entry **5**) was arbitrary set to 1. All compounds were assessed at 10 μM compound concentration for 6 days. The kinase inhibition data represent mean values ± SEM of three independent measurements performed in duplicate. NT, not tested; ND, no IC₅₀ value could be determined under the kinase assay conditions. See also [Table S4](#) and [Table S5](#).

well tolerated. For instance, the *meta*-fluoro derivative **16** (entry **16**) and the *meta*-methyl derivative **17** (entry **17**) were more potent than TR (entry **5**). The *meta*-chloro substitution in derivative **15** (entry **15**) yielded a compound 8-fold more active than the

parent TR. Equipment of the *meta*-position with a methoxy group as shown in derivative **20** (entry **20**), a trifluoromethyl-group in derivative **19** (entry **19**), or an amino group in derivative **21** (entry **21**) led to reduced activity. Substitution of the *ortho*-position was

tolerated as well and TR analogs with an *ortho*-fluoro substituent as in derivative **23** (entry **23**) and an *ortho*-methoxy group in derivative **22** (entry **22**) exhibited activities comparable with the initial hit TR (entry **5**). Overall, the structure-activity relationship revealed that modifications in *meta*- and *ortho*-positions are tolerated and may lead to increased activity, whereas even a minor structural change at the *para*-position nearly abolished the conversion efficiency. Given this strong influence of phenyl mono-derivatization on the reprogramming efficiency, various di-substituted derivatives were generated (entries **24–28**, Table 1). Two *ortho*-fluorine or chlorine atoms in derivatives **27** and **24**, respectively (entries **27** and **24**), are beneficial for reprogramming activity compared with TR (entry **5**). However, the introduction of two chlorines in *para*- and *meta*-position as shown for derivative **26** (entry **26**) only slightly increased the reprogramming efficiency, which is in agreement with the observations made for the monosubstituted analogs, i.e., the positive influence of the *meta*-chloro substituent is negatively balanced by the large *para*-substituent.

In general, the phenyl ring is important for reprogramming activity as shown by the results recorded for derivatives **29–33** (entries **29–33**, Table 1) since replacement with different heterocycles led to reduced activity. Only the introduction of a 1-naphthyl moiety as for compound **29** (entry **29**) yielded an agent more active than TR. In addition, replacement of the amino group adjacent to the phenyl ring by different substituents negatively affects the desired biological activity as indicated by the results obtained for compounds **34–36** (entries **34–36**, Table 1). Moreover, we investigated compounds that contain either a methyl or a thiomethyl group in position C2 (entries **37–40**, Table 1). Derivatives **37** and **39** (entries **37** and **39**) were completely inactive in the reprogramming assay. In addition, we generated a set of compounds that maintain the two substitutions in position C2 but are equipped in the *meta*-position of the phenyl ring with a fluorine atom (entries **38** and **40**). By analogy to the findings described above, only the addition of a fluorine atom in the case of thiomethyl derivative **40** (entry **40**) increased the reprogramming efficiency (compare entry **37** with entries **39–40**).

Thus, the structure-activity relationship study indicated that the range of allowed alterations at positions C6 and C7 of the pteridine scaffold is limited to selected modifications on the phenyl ring and that the adjacent amino group needs to be kept. In addition, the amino group in position C2 is important and can be replaced with thiomethyl only if a fluorine atom is introduced in the *meta*-position of the C6 phenyl ring. However, this compound was less efficient than the parent C2 amino substituted congener (Figure 3C highlights the allowed substitutions on the pteridine ring that control the reprogramming activity).

As described above, compounds **15**, **16**, **29**, **24**, and **26** exhibited an increased biological activity compared with TR (see chemical structures in Figure 3D). Since these compounds reprogram EpiSCs, we term them Epiblastins and sublabel them according to decreasing reprogramming efficiency as Epiblastins A–E, i.e., the most potent compound **15** is termed Epiblastin A (see chemical structure in Figure 3D).

Small chemical modifications of kinase inhibitors were reported to alter their enzymatic inhibition profiles (Miduturu et al., 2011; Goldstein et al., 2008). Therefore, we investigated

the impact of a chlorine atom in the *meta*-position of TR on kinase inhibition and profiled Epiblastin A under the same conditions as TR employing the same kinase panel. On the one hand, the results showed that Epiblastin A has a kinase inhibition profile similar to TR (see Table S3), indicating a similar inhibition mechanism. On the other hand, we observed a stronger inhibition of the CK1 $\alpha/\delta/\epsilon$ isoenzymes (see Figure 3E and compare Figure 2B with Figure 3E). This finding was further confirmed by dose-dependent inhibition studies that yielded IC₅₀ values of 3.8 μ M, 0.8 μ M, and 3.7 μ M for CK1 α , CK1 δ , and CK1 ϵ , respectively (see Figure 3F). This observation suggests that a higher degree of CK1 family inhibition qualitatively correlates with increased reprogramming efficiency observed for Epiblastin A compared with TR.

Modifications on the Pteridine Scaffold Yield Potent and/or Selective CK1 Inhibitors

To assess the potential contribution on the individual isoforms to the conversion, the compound collection described above was investigated for inhibition of human CK1 δ and ϵ by means of an assay employing the KinaseGlo reagent (Promega). From the inhibition assays (entries **5–40**, Table 1 and Table S4; entries **50–59**, Table S5) the following insights were gleaned:

1. Compared with TR (entry **1**, Table 1), introduction of a substituent into the *para*-position of the phenyl ring at C6 of the pteridine core is detrimental to inhibition of CK1 δ/ϵ (compare entry **5** with entries **6–14**).
2. The *meta*-substituent at the C6 phenyl ring greatly affects the kinase inhibitory activity (compare entry **5** with entries **15–21**). In line with the potency observed in the reprogramming assay, Epiblastin A (entry **15**) was identified as the most potent CK1 δ inhibitor. Replacement of the *meta*-chlorine by bromine only slightly reduced activity, whereas in the presence of fluorine the activity was nearly abolished (compare entry **15** with entries **18** and **16**). Replacement of the *meta*-chlorine by a methoxy, methyl, or amino group yielded analogs with lower potency (compare entry **15** with entries **20**, **17**, and **21**). By analogy, Epiblastin A (entry **15**) was also the most potent CK1 ϵ inhibitor identified across the series, however, this isoenzyme was inhibited with an IC₅₀ ca. 10 times higher than the IC₅₀ value determined for CK1 δ .
3. Among the 6-phenyl di-substituted derivatives, selectivity for the CK1 ϵ isoenzyme can be achieved. Thus, compound **25** (entry **25**) containing chlorine atoms in the *ortho*- and *para*-positions of the phenyl ring emerged as a fairly potent and selective CK1 ϵ inhibitor (IC₅₀ = 4.3 μ M for CK1 ϵ ; upon treatment with 50 μ M compound **25**, 44% residual CK1 δ activity was measured). None of the remaining derivatives tested within this series inhibited CK1 δ or yielded more potent inhibitors of CK1 ϵ (compare entry **15** with entries **24–28**).
4. Replacement of the phenyl ring at C6 by heterocycles in general does not improve the potency of CK1 δ inhibition (entries **29–33**). However, introduction of a 1-naphthyl group as in Epiblastin C (entry **29**) instead of a phenyl ring yielded an inhibitor that displayed an IC₅₀ value of 1 μ M for CK1 ϵ and 36 μ M for CK1 δ . Thus, Epiblastin C

(entry **29**) is one of the most selective CK1 ϵ inhibitors among the CK1 δ/ϵ isoenzymes (Walton et al., 2009). Good selectivity was also observed in the case of derivative **30** (entry **30**), containing a 2-pyridyl substituent. In addition, compound **31** (entry **31**) containing a benzo[b]thiophen-3-yl moiety yielded the most potent CK1 ϵ inhibitor among the series with an IC₅₀ value of 0.6 μ M.

- Removal of the amino group at C7 leads to selectivity for CK1 ϵ as shown by derivative **35** (entry **35**), whereas substitution of the amino group at C7 with a phenyl ring in compound **34** (entry **34**) yields an inactive agent. Surprisingly, addition of a 3-hydroxyphenyl substituent to C6 and C7 as in derivative **36** (entry **36**, also known as TG100-115) restored the inhibitory activity against both CK1 δ and ϵ isoenzymes.
- Replacement of the amino group at C2 of the pteridine scaffold leads to complete loss of CK1 inhibiting activity regardless of the investigated isoenzyme or the phenyl ring substitution pattern at position C6 as shown by derivatives **37–40** (entries **37–40**, Table 1).
- Replacement of the amino group at C4 of Epiblastin A (entry **15**) with various alkoxy substituents (see synthesis procedure in Figure S2A) completely abolishes inhibitory activity against CK1 δ (see entries **50–59**, Table S5), suggesting that the presence of the amino group as an H-bond-donating moiety is essential for the inhibitory activity.

A selected number of derivatives were tested for the inhibition of the closely related CK1 α isoform (see Table 1). Apparently, only a few derivatives proved to be potent inhibitors of this isoenzyme. Thus, Epiblastin A and derivatives **18**, **31**, **36** (entries **15**, **18**, **31**, and **36**) exhibit IC₅₀ values for inhibition of CK1 α below 10 μ M, while the compounds **16**, **25**, **29**, and **35** (entries **16**, **25**, **29**, and **35**) show IC₅₀ values higher than 30 μ M.

Taken together, appropriate adjustment of the substitution pattern on the pteridine ring in various positions allowed the generation of potent and/or selective CK1 $\alpha/\delta/\epsilon$ inhibitors. For example, *meta*-substitution with a chlorine atom yielded selective CK1 δ inhibitors as shown in the case of Epiblastin A (entry **15**). Interestingly, a bromine atom in the same position furnished a pan-CK1 α/δ inhibitor (entry **18**), whereas derivatives **25**, **30**, **35**, and Epiblastin C (entries **25**, **30**, **35**, and **29**, respectively) were selective CK1 ϵ inhibitors. We stress that Epiblastin A (entry **15**) and Epiblastin C (entry **29**) are selective CK1 δ /CK1 ϵ inhibitors (Peifer et al., 2009; Richter et al., 2014; Mashhoon et al., 2000) that may open up novel avenues for the study of CK1-isoenzyme modulated processes.

In order to determine the inhibition type, Epiblastin A (entry **15**) was assayed for CK1 δ/ϵ inhibition in the presence of different ATP concentrations. A Lineweaver-Burk plot clearly revealed that this compound is an ATP competitive inhibitor (see Figure 4A–B). The inhibition mode was also confirmed by the inhibition profiles at different ATP concentrations (see Figures S2B and S2C). Moreover, a Dixon plot revealed an inhibition constant (K_i) for CK1 δ of 0.86 μ M and 3.71 μ M for CK1 ϵ (see Figures 4C and 4D). This inhibition mode is also in accordance with the observation that the C2 and C4 amino groups at the pteridine scaffold are required for activity. Determination of crystal struc-

tures of CK1 δ in complex with Epiblastin A and derivative **18** (entries **15** and **18**, Table 1, PDB: 5IH5 and 5IH6) at 2.56 Å and 2.76 Å resolution, respectively, revealed that the 2,4-diaminopyrimidine unit forms an array of H bonds within the nucleotide binding site. The two compounds differ only in the halogen substituent present in the *meta*-position of the phenyl ring at position C6, i.e., a chlorine atom in Epiblastin A and a bromine atom in derivative **18**. As shown in Figure 4E, the amino group in position C2 is engaged in two H bonds with the carbonyl groups of Leu85 and Gly86. Moreover, the amino group at position C4 points to the carbonyl moiety of Glu83. The interaction of the inhibitors with the hinge region is enforced by the fourth H bond between the nitrogen at position 3 and the NH residue of Leu85. Finally, the *meta*-halogen substituent on the C6 phenyl ring is deeply buried inside a hydrophobic cavity created by Met80 and Met82. The position of the bromine atom in derivative **18** has specifically been located inside the ATP-binding pocket of CK1 δ via its characteristic anomalous X-ray scattering signal (see Figure S2D). Due to the strong X-ray absorbance of heavy atoms like bromine, atom-specific anomalous density can be observed if the wavelength of the X-ray is adjusted to the characteristic absorption edge, 0.91883 Å in the case of bromine. Comparison with other CK1 $\delta/\epsilon/\gamma$ -ligand structures present in the protein database (PDB) shows that most inhibitors use a similar binding mode exhibiting hydrogen bridges to the hinge region (Glu83 to Gly86) and hydrophobic interactions in a deeply buried pocket formed by amino acid residues Met80 and Met82. For example, the pan-CK1 δ/ϵ inhibitor PF670462 (PDB: 3UYT and 3UZP, respectively) is protruding even deeper in this cavity than Epiblastin A (Long et al., 2012a, 2012b). The interaction of Epiblastin A with the nucleotide binding pocket of CK1 δ confirms the conclusions of the enzymatic study (see Table 1). Thus, the proper interaction with the hydrophobic cavity is mandatory for a high degree of CK1 δ inhibition (see entries **15–21**, Table 1). Moreover, any derivatization of the *para*-position would potentially clash into the Glu52/Met80 residues found in close proximity (see entries **5–14**, Table 1). Not even the introduction of a *meta*-chloro substitution on the *para*-chlorine-containing derivative as shown for compound **26** (entry **26**) could block the enzymatic activity of CK1 δ/ϵ isoforms. Together, these observations clearly suggest restricted functionalization possibilities of the phenyl ring at position C6. Although the *ortho-para*-chlorine disubstitution as shown for derivative **25** (entry **25**) yielded an inactive compound against CK1 δ , this derivative exhibited an IC₅₀ value of approximately 4.3 μ M for the CK1 ϵ isoenzyme. The result suggests that this precise arrangement of substituents can be exploited to generate CK1 ϵ -selective inhibitors.

Target Engagement in Cell Lysates

Target engagement (Simon et al., 2013) in cell lysates was investigated by means of a kinase enrichment assay employing an ActivX ATP probe (Thermo Fisher; <https://www.thermofisher.com/order/catalog/product/88310>.) that features a desthiobiotin-bearing mixed carboxylic/phosphoric acid anhydride at the γ -phosphate position of the ATP. When bound to a kinase ATP-binding site, the desthiobiotin moiety is transferred to a proximal ϵ -amino group of a lysine residue (Rosenblum et al., 2013; Saraste et al., 1990; Deyrup et al., 1998), and labeled kinases can be enriched by means of streptavidin and subsequently detected

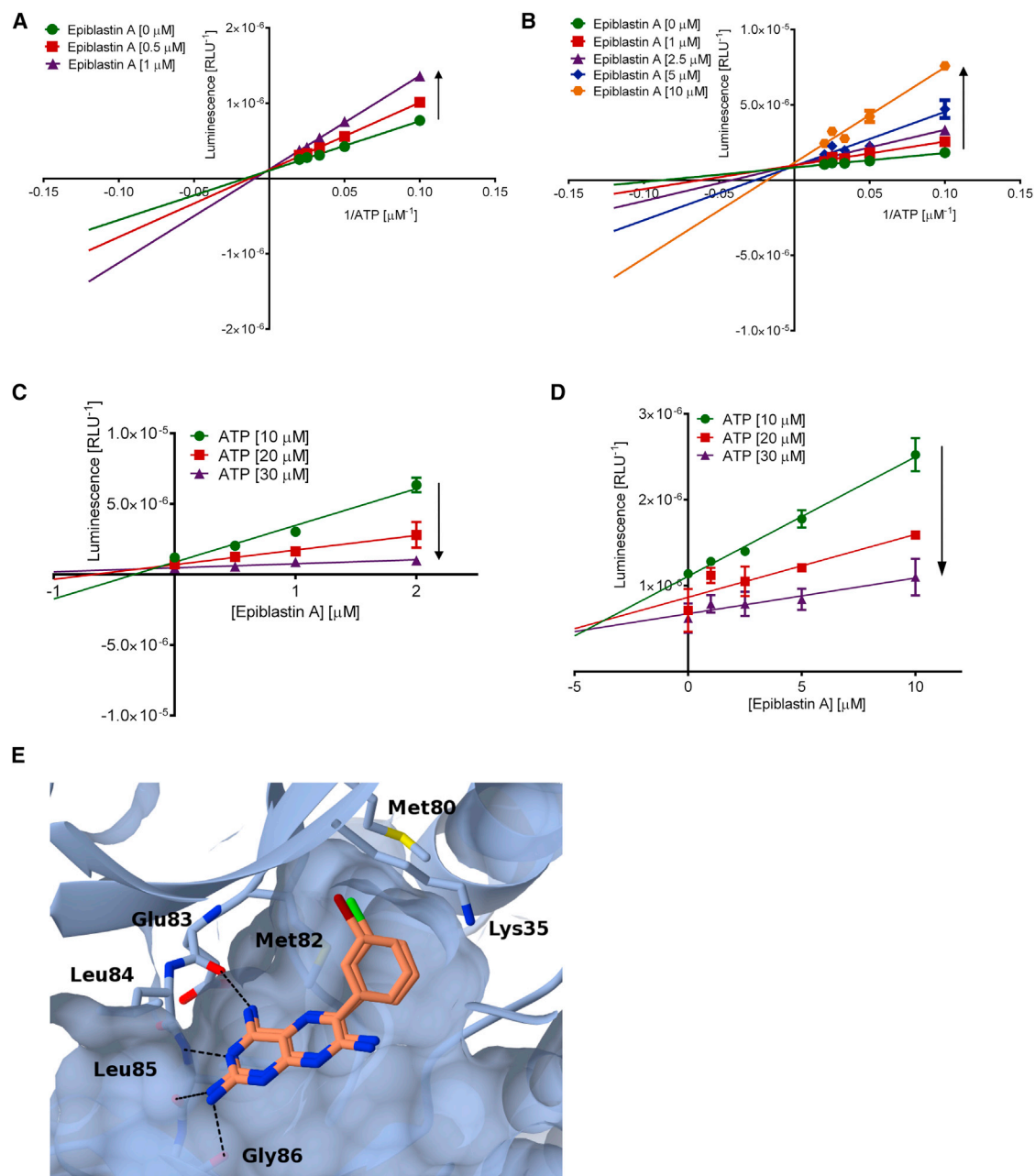


Figure 4. Epiblastin A is an ATP Competitive Inhibitor of CK1 δ/ϵ Isoenzymes

(A) A Lineweaver-Burk plot shows competitive inhibition of CK1 δ by Epiblastin A with respect to various concentrations of ATP. Data represent mean values \pm SEM of three independent measurements performed in duplicate. Black arrows indicate the increasing concentrations of Epiblastin A.

(B) A Lineweaver-Burk plot shows competitive inhibition of CK1 ϵ by Epiblastin A with respect to various concentrations of ATP. Data represent mean values \pm SEM of three independent measurements performed in duplicate. Black arrows indicate the increasing concentrations of Epiblastin A.

(C) A Dixon plot for CK1 δ yields the inhibition constant for Epiblastin A by using different concentrations of Epiblastin A at various ATP concentrations. Data represent mean values \pm SEM of three independent measurements performed in duplicate. Black arrows indicate the increasing concentrations of ATP.

(D) A Dixon plot for CK1 ϵ yields the inhibition constant for Epiblastin A by using different concentrations of Epiblastin A at various ATP concentrations. Data represent mean values \pm SEM of three independent measurements performed in duplicate. Black arrows indicate the increasing concentrations of ATP.

(E) Crystal structures of Epiblastin A and derivative **18** in complex with CK1 δ . The chlorine atom in Epiblastin A is shown in green, while the bromine in derivative **18** is highlighted in brown. Nitrogen and carbon atoms are depicted in blue and red, respectively. The four hydrogen bonds between the hinge region and the 2,4-diaminopyrimidine unit of Epiblastin A and derivative **18** are shown as black dashed lines.

RLU, relative light units. See also Figure S2.

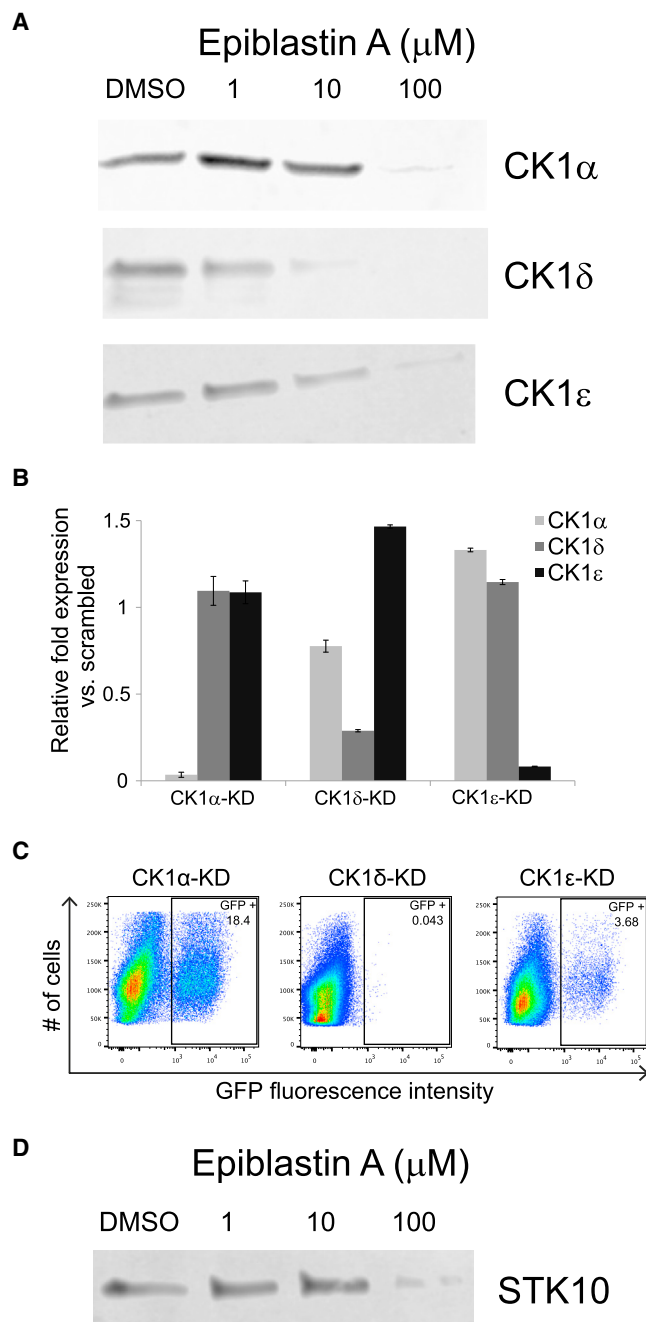


Figure 5. Target Confirmation Studies of Epiblastin A in HCT116 Cell Lysate

(A) Epiblastin A disturbs the labeling of CK1 α , CK1 δ , CK1 ϵ isoenzymes in HCT116 cell lysates. Nucleotide-depleted lysates of HCT116 cells were incubated with different concentrations of Epiblastin A or DMSO as a control for 10 min followed by treatment with ActivX ATP probe for 10 min. Labeled proteins were enriched using streptavidin beads and were separated by means of SDS-PAGE. Proteins were transferred to a polyvinylidene fluoride (PVDF) membrane prior to detection of CK1 $\alpha/\delta/\epsilon$ using anti-CK1 α , anti-CK1 δ , and anti-CK1 ϵ antibody and secondary antibodies coupled to horseradish peroxidase. Data are representative of three independent experiments.

(B) Assessment of CK1 shRNA-based knockdown efficiency in E3 GOF18-EpiSCs cells by quantitative PCR analysis. Data represent mean values \pm SEM of three independent measurements.

by western blotting. Inhibition of probe binding leads to reduced labeling and thereby weaker bands in the immunoblot. Short incubation times and low probe concentrations minimize unspecific lysine labeling (Okerberg et al., 2009). The robustness of the method for analysis of ATP-binding proteins, in particular kinases, has previously been proven (Xiao and Wang, 2014; Patri-cell et al., 2011; McAllister et al., 2013; Adachi et al., 2014). One of the advantages of this technology is that appendage of a linker is not required. The nature of the linker and its attachment position on a scaffold of a linker can affect activity (Ziegler et al., 2013). Target engagement by Epiblastin A was investigated in human HCT116 colorectal carcinoma cells because all CK1 isoenzymes could be detected in the cell lysate (see Figure S3A). After incubation of the HCT116 cell lysate with increasing concentrations of Epiblastin A (1, 10, and 100 μM , respectively) and addition of the probe, labeled proteins were isolated using streptavidin-coated beads and analyzed by means of immunoblotting. As shown in Figure 5A, in the absence of inhibitor, CK1 $\alpha/\delta/\epsilon$ are labeled by the reagent. Addition of Epiblastin A to the cell lysate in increasing concentrations impairs labeling and, therefore, binding of the ATP probe to the kinase. This result proves engagement of the three CK1 $\alpha/\delta/\epsilon$ isoenzymes by Epiblastin A in HCT116 cell lysate. In order to determine whether Epiblastin A binds kinases in addition to the CK1 isoforms, in a separate experiment kinases whose labeling could be inhibited by Epiblastin A were identified and quantified by means of label-free mass spectrometry (see the Supplemental Experimental Procedures and Figure S3B for the list of proteins identified). The analysis revealed CK1 α as target protein in accordance with the findings detailed above. CK1 δ and CK1 ϵ were identified as well, however with lower confidence. Notably, CK1 α could be identified in all replicates of the chemical proteomics experiment, indicating that CK1 α may be the major cellular target of Epiblastin A in HCT116 cell lysate. Having identified the CK1 $\alpha/\delta/\epsilon$ isoenzymes as targets of Epiblastin A, we set out to determine the contribution of each CK1 isoform in the reprogramming process. Therefore, we performed shRNA-mediated knockdown in E3 GOF18-EpiSCs (see Figures 5B and 5C). Genetic ablation of CK1 ϵ and mainly the CK1 α isoenzyme yielded 4% and 18% GFP-positive colonies, respectively, as quantified by flow cytometry, suggesting a major contribution of the CK1 α isoform inhibition during reprogramming of EpiSCs.

In addition to CK1 α , serine/threonine-protein kinase 10 (STK10) (Kuramochi et al., 1997) was detected in the proteomics experiment to bind to Epiblastin A (see Figure S3B). An in vitro enzymatic assay revealed that Epiblastin A indeed inhibits

(C) Oct4-GFP expression in E3 GOF18-EpiSCs after shRNA-based knockdown of CK1 α , CK1 δ , and CK1 ϵ as measured by flow cytometry. The cells were cultured in conditioned EpiSC medium containing FGF2 and Activin A. Data are representative of three independent experiments.

(D) Epiblastin A disturbs the labeling of STK10 in HCT116 cell lysates. Nucleotide-depleted lysates of HCT116 cells were incubated with different concentrations of Epiblastin A or DMSO as a control for 10 min followed by treatment with ActivX ATP probe for 10 min. Labeled proteins were enriched using streptavidin beads and were separated by means of SDS-PAGE. Proteins were transferred to a PVDF membrane prior to detection of STK10 using anti-STK10 antibody and secondary antibody coupled to horseradish peroxidase. Data are representative of three independent experiments. See also Figure S3 and Figure S4.

STK10 kinase activity with an IC_{50} value of 19 μ M (see [Figure S3C](#)). By analogy to the method described above, immunoblotting proved engagement of Epiblastin A by STK10 (see [Figure 5D](#)) in lysates obtained from HCT116 cells.

The chemical proteomics approach identified phosphatidylinositol-5-phosphate 4-kinases type 2 ([Fiume et al., 2015](#)), kinases PIP4K2A and PIP4K2C, as putative targets (see [Figure S3B](#)). Given the fact that TR analog TG100-115 ([Palanki et al., 2007](#)) had been identified as an inhibitor of PI3Ks before ([Davis et al., 2011](#); [Doukas et al., 2006](#)), this result may represent a more general affinity of the pteridine chemotype for lipid kinases. In light of these findings, Epiblastin A was subjected to an additional kinase profiling study monitoring a total of 123 kinases (see [Table S6](#)). The analysis revealed that it further inhibits brain-selective kinase 1 (BRSK1; IC_{50} = 24.2 \pm 5.8 μ M), eukaryotic elongation factor 2 kinase (EEF2K; IC_{50} = 27.4 \pm 5.6 μ M), epidermal growth factor receptor kinase (EGFR; IC_{50} = 8.3 \pm 1.5 μ M), Map kinase-interacting Ser/Thr kinase 2 (MKNK2; IC_{50} = 45.0 \pm 10.3 μ M), and receptor-interacting Ser/Thr kinase 2 (RIPK2; IC_{50} = 38.0 \pm 11.3 μ M) (see [Figures S4A–S4F](#)). While these data might be considered in the rationalization of the stem cell reprogramming activity of Epiblastin A, inhibition of these kinases is much weaker than for the CK1 isoenzymes (with the possible exception of EGFR; see the Discussion below) and may, therefore, not be relevant under the conditions of the reprogramming experiments. Further studies are required to clarify this possibility.

DISCUSSION

Chemical reprogramming of differentiated cells into PSCs is an emerging technology that may enable the identification and interrogation of the cellular pathways that govern stem cell dedifferentiation ([Boiani and Scholer, 2005](#); [Ng and Surani, 2011](#)). We describe the identification of the initial hit compound TR discovered in a cell-based assay monitoring the efficient reactivation of Oct4-GFP expression in mouse EpiSCs. The synthesis of a collection of TR analogs yielded Epiblastins A–E as a class of pteridine compounds that efficiently and reproducibly converted EpiSCs to cESCs that re-express the Oct4-GFP transgene and exhibit cell morphology similar to ESCs. Variation of the substitution pattern at different positions of the pteridine ring furnished potent and/or selective CK1 α / δ / ϵ inhibitors. Epiblastin A and Epiblastin C are excellent candidates for further improvement of inhibitory activity and/or selectivity toward CK1 δ and CK1 ϵ , respectively. The crystal structures obtained for Epiblastin A and derivative **18** in complex with the target protein provide a solid structural basis for these studies.

The data generated from the cell-based assays, the inhibition studies, and analysis of target engagement indicate that for the most potent compound identified, i.e., Epiblastin A, inhibition of CK1 α may be the most relevant activity for EpiSC reprogramming. However, acquiring ESC-like features in the case of EpiSCs is possible via a CK1 independent mechanism as well. Recent findings suggest that EpiSC lines of various origins can be converted to an ESC-like state by genetic and/or chemical manipulation of different targets ([Bao et al., 2009](#); [Gillich et al., 2012](#); [Zhou et al., 2010](#); [Festuccia et al., 2012](#); [Bernemann et al., 2011](#); [Yang et al., 2010](#); [Guo et al., 2009](#)).

Analysis of target engagement by means of chemical proteomics indicated that also other kinases inhibited by Epiblastin A may be involved in the reprogramming process. However, of the enzymes for which binding was confirmed, only CK1 α has been previously linked to stem cell biology as a regulator of the DNA damage response in mouse ESCs ([Carreras Puigvert et al., 2013](#)). CK1 α inhibition has not been described as a critical step in EpiSC reprogramming before, although kinome-wide RNAi and kinase inhibitors screens have been performed in the past ([Sakurai et al., 2014](#); [Lee et al., 2012](#)). Thus, our chemical proteomics approach may have revealed possible novel targets that might act as reprogramming barriers in the stem cell context and could not be identified by means of genome-wide RNAi screens before ([Yang et al., 2014](#); [Qin et al., 2014](#)).

In vitro kinase profiling revealed additional proteins potentially targeted by Epiblastin A in cells. However, with the exception of the EGFR kinase, the IC_{50} values for their inhibition were considerably higher than for the CK1 isoenzymes, in particular CK1 α . Thus, it appears unlikely that inhibition of these kinases plays a decisive role in stem cell reprogramming. Notably, a recent literature report ([Tran et al., 2015](#)) characterizes EGF receptor components as barriers in the transition from the pre-cESC to the ESC-like state. Thus, [Tran et al. \(2015\)](#) found that reduction of EGFR kinase levels at the later stages of reprogramming facilitated the transition to the ESC-like state via activation of Esrrb expression, an important component of the pluripotency network ([Festuccia et al., 2012](#); [Feng et al., 2009](#)).

Epiblastin A is a valuable tool compound to further identify and characterize the signaling events involved in the conversion of EpiSCs into an Oct4-GFP expressing cell population (D.J.I., M.Z., A.U., S.Z., H.W., H.R.S., and colleagues, unpublished data). Given the identification of CK1 α as a major determinant of this activity, further compound improvement by means of a structure-based inhibitor design may allow the development of more potent and selective modulators of stem cell fate.

SIGNIFICANCE

Novel small molecules that influence stem cell reprogramming are in high demand because they may pave the way for new therapeutic applications and be efficient tools to unravel the cellular networks that govern stem cell renewal and differentiation. Conversion of mammalian epiblast stem cells (EpiSCs) characterized by primed pluripotency into cells corresponding to embryonic stem cells (cESCs) by means of established techniques is ineffective because only a minority of EpiSCs (1% or even less) is converted. The application of Epiblastin A now allows for efficient reprogramming of EpiSCs into cESCs and thereby enables their further use. The identification of casein kinases as primary cellular targets of Epiblastin A revealed that these enzymes are important factors in the cellular networks determining pluripotency. The results suggest that regulation of casein kinase 1 α (CK1 α) enzymatic activity is a critical step in EpiSC reprogramming. This kinase family represents an important reprogramming barrier in the stem cell context not identified by genome-wide RNAi screens before. The development of an efficient synthesis of a triamterene-derived compound collection, the delineation of a

conclusive structure-activity relationship, and the availability of crystal structures of Epiblastin A in complex with CK1 δ enable further inhibitor improvement for in-depth analysis of the signaling pathways that govern stem cell dedifferentiation and better manipulation of stem cell fate in vitro.

EXPERIMENTAL PROCEDURES

General Procedure for the Synthesis of Derivatives 5–40

Epiblastin A (entry 15): NaH (60% oil dispersion, 0.75 mmol, 1.1 eq) was dissolved in 8 ml of anhydrous 2-ethoxyethanol and vigorously stirred at room temperature. After H₂ evolution, a clear solution was obtained and then (3-chlorophenyl)acetonitrile (0.75 mmol, 1.1 eq) was added followed by 5-nitroso-2,4,6-triaminopyrimidine (0.68 mmol, 1 eq). The reaction mixture was heated to 140°C and refluxed for 2 hr. After cooling to room temperature, the mixture was concentrated in vacuo. The solid obtained was treated with 5 ml of water, filtered, and washed twice with 3 ml of methanol. The solid was dried to finally furnish 107 mg of a yellow solid (yield, 55%) (see [Supplemental Experimental Procedures](#) for more details).

Fluorescence-Activated Cell Sorting-Based Detection of GFP-Positive Cells

100,000 E3 EpiSC GOF18 cells were plated into 6 cm low attachment dishes on day 0. The reprogramming assay was performed in EpiSC medium, i.e., CF1 MEF-conditioned KO-DMEM containing 20% serum replacement and without additional bFGF. Compounds were added on day 0 at a concentration of 10 μ M, and cells were incubated for 8 days at 37°C. Medium containing the compounds was changed on days 4 and 6. The basic EpiSC conversion medium was used as negative control, and a mixture of 3 μ M CHIR99021 (GSK3 β inhibitor), 1 μ M PD0325901 (MEK1 inhibitor), and 2000 U/ml LIF (commonly referred to as 2i/LIF) was used as a positive control for reprogramming E3 EpiSC GOF18 cells. On day 8, cells were dissociated using trypsin. Approximately one million cells were resuspended in 500 μ l of cell culture medium and the suspension was passed through a 40 μ m cell strainer to remove debris and undissociated tissue. DAPI was added to stain the nuclei. Cells were subjected to fluorescence-activated cell sorting using a FACSAria cell sorter (BD Biosciences) to detect the selective expression of the Oct4-GFP construct in embryonic stem-like cells, i.e., reprogrammed cells. On day 8 of reprogramming, reverted E3 EpiSCs displayed reactivation of the Oct4-GFP transgene. The yield of conversion was related to the initial hit TR, whose efficiency was set to 1.

Detection of Target Engagement Using the ActivX ATP Probe

HCT116 cells were lysed in ice-cold Pierce IP lysis buffer (25 mM Tris-HCl [pH 7.4], 150 mM NaCl, 1 mM EDTA, 1% NP-40, and 5% glycerol). 10 μ l of 1 M MgCl₂ was added to ca. 1 mg HCT116 cell lysate and samples were incubated for 1 min at room temperature prior to addition of DMSO or Epiblastin A to yield 1, 10, and 100 μ M Epiblastin A. Samples were incubated at room temperature for 10 min. The ActivX ATP probe (Life Technologies) was pre-equilibrated at room temperature prior to incubation with the DMSO and Epiblastin A-treated samples at room temperature for 10 min. The solution was diluted 1:2 in 8 M urea stock solution in Pierce IP lysis buffer, followed by the addition of high-capacity streptavidin agarose resin (Pierce Streptavidin Agarose) and incubation for 1 hr at room temperature. Samples were centrifuged at 1,000 \times g for 1 min and washed twice using 4 M urea in Pierce IP lysis buffer followed by centrifugation at 1,000 \times g for 1 min. Finally, proteins were denatured in 2 \times Laemmli buffer (100 mM Tris [pH 6.8], 7% SDS, 200 mM DTT, 0.014% bromophenol blue). Samples were then analyzed by means of immunoblotting or mass spectrometry (see [Supplemental Experimental Procedures](#) for more details).

For cloning, expression and crystal structure determination, kinase assays, shRNA-mediated knockdown, quantitative PCR, and biochemical procedures, see [Supplemental Experimental Procedures](#).

ACCESSION NUMBERS

The accession numbers for the crystal structures of CK1 δ in the apo form and in complex with Epiblastin A and derivative 18 reported in this paper are PDB: 5IH4, 5IH5, and 5IH6.

SUPPLEMENTAL INFORMATION

Supplemental Information includes Supplemental Experimental Procedures, four figures, and seven tables and can be found with this article online at <http://dx.doi.org/10.1016/j.chembiol.2016.02.015>.

AUTHOR CONTRIBUTIONS

A.U., D.J.I., Y.T., A.T.P., and M.Z. conducted the experiments. A.U. synthesized the pteridine compound collection. D.J.I. designed and performed the stem cell reprogramming assay. A.U. and Y.T. designed and carried out the CK1 enzymatic studies. A.T.P. performed crystallization studies. A.U. performed the target engagement and the chemical proteomics studies. M.Z. carried out the knockdown experiments. A.B., P.J., N.W., H.O., I.R.V., S.Z., H.R.S., and H.W. supervised the project. A.U., S.Z., and H.W. conceived the paper. All authors contributed to writing the manuscript.

ACKNOWLEDGMENTS

A.U. and A.T.P. are International Max Planck Research School of Chemical and Molecular Biology (IMPRS-CMB) fellows. We acknowledge Katrin Murlowski's assistance in the synthesis of derivatives 41–59. We thank the Dortmund Protein Facility (DPF) for CK1 δ and CK1 ϵ plasmid construction, protein expression, and purification. We would like to acknowledge Dr. Raphael Gasper-Schönenbrücher, Susanne Terheyden, Dr. Katja Gotthardt, Dr. Matthias Müller, David Bier, and Stefan Baumeister for collecting the crystallographic data as well as the SLS X10SA beamline staff for their excellent support. The research leading to these results has received funding from the Max Planck Society and the European Research Council under the European Union's Seventh Framework Program (FP7/2007–2013/ERC grant agreement no. 268309).

Received: December 4, 2015

Revised: February 15, 2016

Accepted: February 25, 2016

Published: March 31, 2016

REFERENCES

- Adachi, J., Kishida, M., Watanabe, S., Hashimoto, Y., Fukamizu, K., and Tomonaga, T. (2014). Proteome-wide discovery of unknown ATP-binding proteins and kinase inhibitor target proteins using an ATP probe. *J. Proteome Res.* 13, 5461–5470.
- Bao, S., Tang, F., Li, X., Hayashi, K., Gillich, A., Lao, K., and Surani, M.A. (2009). Epigenetic reversion of post-implantation epiblast to pluripotent embryonic stem cells. *Nature* 461, 1292–1295.
- Bernemann, C., Greber, B., Ko, K., Sternecker, J., Han, D.W., Araújo-Bravo, M.J., and Schöler, H.R. (2011). Distinct developmental ground states of epiblast stem cell lines determine different pluripotency features. *Stem Cells* 29, 1496–1503.
- Boiani, M., and Scholer, H.R. (2005). Regulatory networks in embryo-derived pluripotent stem cells. *Nat. Rev. Mol. Cell Biol.* 6, 872–881.
- Brons, I.G.M., Smithers, L.E., Trotter, M.W.B., Rugg-Gunn, P., Sun, B., Chuva De Sousa Lopes, S.M., Howlett, S.K., Clarkson, A., Ahrlund-Richter, L., Pedersen, R.A., and Vallier, L. (2007). Derivation of pluripotent epiblast stem cells from mammalian embryos. *Nature* 448, 191–195.
- Busch, A.E., Suessbrich, H., Kunzelmann, K., Hipper, A., Greger, R., Waldegger, S., Mutschler, E., Lindemann, B., and Lang, F. (1996). Blockade of epithelial Na⁺ channels by triamterenes - underlying mechanisms and molecular basis. *Pflügers Arch.* 432, 760–766.
- Carreras Puigvert, J., Von Stechow, L., Siddappa, R., Pines, A., Bahjat, M., Haazen, L.C.J.M., Olsen, J.V., Vrieling, H., Meerman, J.H.N., Mullenders, L.H.F., et al. (2013). Systems biology approach identifies the kinase Csnk1a1 as a regulator of the DNA damage response in embryonic stem cells. *Sci. Signal.* 6, ra5.

- Davis, M.I., Hunt, J.P., Herrgard, S., Ciceri, P., Wodicka, L.M., Pallares, G., Hocker, M., Treiber, D.K., and Zarrinkar, P.P. (2011). Comprehensive analysis of kinase inhibitor selectivity. *Nat. Biotechnol.* 29, 1046–1051.
- Deyrup, A.T., Krishnan, S., Cockburn, B.N., and Schwartz, N.B. (1998). Deletion and site-directed mutagenesis of the ATP-binding motif (P-loop) in the bifunctional murine ATP-sulfurylase/adenosine 5'-phosphosulfate kinase enzyme. *J. Biol. Chem.* 273, 9450–9456.
- Doukas, J., Wrasidlo, W., Noronha, G., Dneprovskaya, E., Fine, R., Weis, S., Hood, J., Demaria, A., Soll, R., and Cheresch, D. (2006). Phosphoinositide 3-kinase γ/δ inhibition limits infarct size after myocardial ischemia/reperfusion injury. *Proc. Natl. Acad. Sci. USA* 103, 19866–19871.
- Federation, A.J., Bradner, J.E., and Meissner, A. (2014). The use of small molecules in somatic-cell reprogramming. *Trends Cell Biol.* 24, 179–187.
- Feng, B., Jiang, J., Kraus, P., Ng, J.-H., Heng, J.-C.D., Chan, Y.-S., Yaw, L.-P., Zhang, W., Loh, Y.-H., Han, J., et al. (2009). Reprogramming of fibroblasts into induced pluripotent stem cells with orphan nuclear receptor Esrrb. *Nat. Cell Biol.* 11, 197–203.
- Festuccia, N., Osorno, R., Halbritter, F., Karwacki-Neisius, V., Navarro, P., Colby, D., Wong, F., Yates, A., Tomlinson Simon, R., and Chambers, I. (2012). Esrrb is a direct nanog target gene that can substitute for nanog function in pluripotent cells. *Cell Stem Cell* 11, 477–490.
- Fiume, R., Stijf-Bultsma, Y., Shah, Z.H., Keune, W.J., Jones, D.R., Jude, J.G., and Divecha, N. (2015). PIP4K and the role of nuclear phosphoinositides in tumour suppression. *Biochim. Biophys. Acta* 1851, 898–910.
- Forbes, S.J., and Rosenthal, N. (2014). Preparing the ground for tissue regeneration: from mechanism to therapy. *Nat. Med.* 20, 857–869.
- Gillich, A., Bao, S., Grabole, N., Hayashi, K., Trotter Matthew, W.B., Pasque, V., Magnúsdóttir, E., and Surani, M.A. (2012). Epiblast stem cell-based system reveals reprogramming synergy of germline factors. *Cell Stem Cell* 10, 425–439.
- Goldstein, D.M., Gray, N.S., and Zarrinkar, P.P. (2008). High-throughput kinase profiling as a platform for drug discovery. *Nat. Rev. Drug Discov.* 7, 391–397.
- González, F., Boué, S., and Belmonte, J.C.I. (2011). Methods for making induced pluripotent stem cells: reprogramming à la carte. *Nat. Rev. Genet.* 12, 231–242.
- Greber, B., Wu, G., Bernemann, C., Joo, J.Y., Han, D.W., Ko, K., Tapia, N., Sabour, D., Sternecker, J., Tesar, P., and Schöler, H.R. (2010). Conserved and divergent roles of FGF signaling in mouse epiblast stem cells and human embryonic stem cells. *Cell Stem Cell* 6, 215–226.
- Grskovic, M., Javaherian, A., Strulovici, B., and Daley, G.Q. (2011). Induced pluripotent stem cells — opportunities for disease modelling and drug discovery. *Nat. Rev. Drug Discov.* 10, 915–929.
- Guo, G., Yang, J., Nichols, J., Hall, J.S., Eyres, I., Mansfield, W., and Smith, A. (2009). Klf4 reverts developmentally programmed restriction of ground state pluripotency. *Development* 136, 1063–1069.
- Han, D.W., Tapia, N., Joo, J.Y., Greber, B., Araúzo-Bravo, M.J., Bernemann, C., Ko, K., Wu, G., Stehling, M., Do, J.T., and Schöler, H.R. (2010). Epiblast stem cell subpopulations represent mouse embryos of distinct pregastrulation stages. *Cell* 143, 617–627.
- Hanna, J., Markoulaki, S., Mitalipova, M., Cheng, A.W., Cassady, J.P., Staerk, J., Carey, B.W., Lengner, C.J., Foreman, R., Love, J., et al. (2009). Metastable pluripotent states in NOD-mouse-derived ESCs. *Cell Stem Cell* 4, 513–524.
- Hou, P., Li, Y., Zhang, X., Liu, C., Guan, J., Li, H., Zhao, T., Ye, J., Yang, W., Liu, K., et al. (2013). Pluripotent stem cells induced from mouse somatic cells by small-molecule compounds. *Science* 341, 651–654.
- Huangfu, D., Maehr, R., Guo, W., Eijkelenboom, A., Snitow, M., Chen, A.E., and Melton, D.A. (2008). Induction of pluripotent stem cells by defined factors is greatly improved by small-molecule compounds. *Nat. Biotechnol.* 26, 795–797.
- Jerabek, S., Merino, F., Schöler, H.R., and Cojocar, V. (2014). OCT4: dynamic DNA binding pioneers stem cell pluripotency. *Biochim. Biophys. Acta* 1839, 138–154.
- Kejin, H. (2014). All roads lead to induced pluripotent stem cells: the technologies of iPSC generation. *Stem Cells Dev.* 23, 1285–1300.
- Kellenberger, S., Gautschi, I., and Schild, L. (2003). Mutations in the epithelial Na⁺ channel ENaC outer pore disrupt amiloride block by increasing its dissociation rate. *Mol. Pharmacol.* 64, 848–856.
- Kuramochi, S., Moriguchi, T., Kuida, K., Endo, J., Semba, K., Nishida, E., and Karasuyama, H. (1997). LOK is a novel mouse STE20-like protein kinase that is expressed predominantly in lymphocytes. *J. Biol. Chem.* 272, 22679–22684.
- Lee, D.-F., Su, J., Ang, Y.-S., Carvajal-Vergara, X., Mulero-Navarro, S., Pereira Carlos, F., Gingold, J., Wang, H.-L., Zhao, R., Sevilla, A., et al. (2012). Regulation of Embryonic and induced pluripotency by aurora kinase-p53 signaling. *Cell Stem Cell* 11, 179–194.
- Long, A., Zhao, H., and Huang, X. (2012a). Structural basis for the interaction between casein kinase 1 delta and a potent and selective inhibitor. *J. Med. Chem.* 55, 956–960.
- Long, A.M., Zhao, H., and Huang, X. (2012b). Structural basis for the potent and selective inhibition of casein kinase 1 epsilon. *J. Med. Chem.* 55, 10307–10311.
- Lunn, J.S., Sakowski, S.A., and Feldman, E.L. (2014). Concise review: stem cell therapies for amyotrophic lateral sclerosis: recent advances and prospects for the future. *Stem Cells* 32, 1099–1109.
- Mashhoon, N., Demaggio, A.J., Tereshko, V., Bergmeier, S.C., Egli, M., Hoekstra, M.F., and Kuret, J. (2000). Crystal structure of a conformation-selective casein Kinase-1 inhibitor. *J. Biol. Chem.* 275, 20052–20060.
- McAllister, F.E., Niepel, M., Haas, W., Huttlin, E., Sorger, P.K., and Gygi, S.P. (2013). Mass Spectrometry based method to increase throughput for kinome analyses using ATP probes. *Anal. Chem.* 85, 4666–4674.
- Miduturu Chandrasekhar, V., Deng, X., Kwiatkowski, N., Yang, W., Brault, L., Filippakopoulos, P., Chung, E., Yang, Q., Schwaller, J., Knapp, S., et al. (2011). High-throughput kinase profiling: a more efficient approach toward the discovery of new kinase inhibitors. *Chem. Biol.* 18, 868–879.
- Ng, H.-H., and Surani, M.A. (2011). The transcriptional and signalling networks of pluripotency. *Nat. Cell Biol.* 13, 490–496.
- Nichols, J., and Smith, A. (2009). Naive and primed pluripotent states. *Cell Stem Cell* 4, 487–492.
- Okerberg, E., Shih, A., Brown, H., Alemayehu, S., Aban, A., and Nomanbhoy, T.K. (2009). Profiling native kinases by immuno-assisted activity-based profiling. *Curr. Protoc. Chem. Biol.* 5, 213–226.
- Osdene, T.S., Russell, P.B., and Rane, L. (1967). 2,4,7-Triamino-6-ortho-substituted arylpteridines. A new series of potent antimalarial agents. *J. Med. Chem.* 10, 431–434.
- Palanki, M.S.S., Dneprovskaya, E., Doukas, J., Fine, R.M., Hood, J., Kang, X., Lohse, D., Martin, M., Noronha, G., Soll, R.M., et al. (2007). Discovery of 3,3'-(2,4-diaminopteridine-6,7-diyl)diphenol as an isozyme-selective inhibitor of PI3K for the treatment of ischemia reperfusion injury associated with myocardial infarction. *J. Med. Chem.* 50, 4279–4294.
- Patricelli, M.P., Nomanbhoy, T.K., Wu, J., Brown, H., Zhou, D., Zhang, J., Jagannathan, S., Aban, A., Okerberg, E., Herring, C., et al. (2011). In situ kinase profiling reveals functionally relevant properties of native kinases. *Chem. Biol.* 18, 699–710.
- Peifer, C., Abadleh, M., Bischof, J., Hauser, D., Schattell, V., Hirner, H., Knippschild, U., and Laufer, S. (2009). 3,4-Diaryl-isoxazoles and -imidazoles as potent dual inhibitors of p38 α mitogen activated protein kinase and casein kinase 1 δ . *J. Med. Chem.* 52, 7618–7630.
- Qin, H., Diaz, A., Blouin, L., Lebbink, R.J., Patena, W., Tanbun, P., Leproust, E.M., Mcmanus, M.T., Song, J.S., and Ramalho-Santos, M. (2014). Systematic identification of barriers to human iPSC generation. *Cell* 158, 449–461.
- Radziszewska, A., and Silva, J.C.R. (2014). Do all roads lead to Oct4? the emerging concepts of induced pluripotency. *Trends Cell Biol.* 24, 275–284.
- Rena, G., Bain, J., Elliott, M., and Cohen, P. (2004). D4476, a cell-permeant inhibitor of CK1, suppresses the site-specific phosphorylation and nuclear exclusion of FOXO1a. *EMBO Rep.* 5, 60–65.

- Richter, J., Bischof, J., Zaja, M., Kohlhof, H., Othersen, O., Vitt, D., Alscher, V., Pospiech, I., García-Reyes, B., Berg, S., et al. (2014). Difluoro-dioxolo-benzimidazol-benzamides as potent inhibitors of CK1 δ and ϵ with nanomolar inhibitory activity on cancer cell proliferation. *J. Med. Chem.* 57, 7933–7946.
- Rosenblum, J.S., Nomanbhoy, T.K., and Kozarich, J.W. (2013). Functional interrogation of kinases and other nucleotide-binding proteins. *FEBS Lett.* 587, 1870–1877.
- Sakurai, K., Talukdar, I., Patil, V.S., Dang, J., Li, Z., Chang, K.-Y., Lu, C.-C., Delorme-Walker, V., Dermardirossian, C., Anderson, K., et al. (2014). Kinome-wide functional analysis highlights the role of cytoskeletal remodeling in somatic cell reprogramming. *Cell Stem Cell* 14, 523–534.
- Saraste, M., Sibbald, P.R., and Wittinghofer, A. (1990). The P-loop — a common motif in ATP- and GTP-binding proteins. *Trends Biochem. Sci.* 15, 430–434.
- Shenghui, H., Nakada, D., and Morrison, S.J. (2009). Mechanisms of stem cell self-renewal. *Annu. Rev. Cell Dev. Biol.* 25, 377–406.
- Shi, Y., Despons, C., Do, J.T., Hahm, H.S., Schöler, H.R., and Ding, S. (2008). Induction of pluripotent stem cells from mouse embryonic fibroblasts by Oct4 and Klf4 with small-molecule compounds. *Cell Stem Cell* 3, 568–574.
- Simon, G.M., Niphakis, M.J., and Cravatt, B.F. (2013). Determining target engagement in living systems. *Nat. Chem. Biol.* 9, 200–205.
- Spickett, R.G.W., and Timmis, G.M. (1954). The synthesis of compounds with potential anti-folic acid activity. Part I. 7-Amino- and 7-hydroxy-pteridines. *J. Chem. Soc.* 2887–2895.
- Sternecker, J.L., Reinhardt, P., and Scholer, H.R. (2014). Investigating human disease using stem cell models. *Nat. Rev. Genet.* 15, 625–639.
- Takahashi, K., and Yamanaka, S. (2006). Induction of pluripotent stem cells from mouse embryonic and adult fibroblast cultures by defined factors. *Cell* 126, 663–676.
- Tesar, P.J., Chenoweth, J.G., Brook, F.A., Davies, T.J., Evans, E.P., Mack, D.L., Gardner, R.L., and McKay, R.D.G. (2007). New cell lines from mouse epiblast share defining features with human embryonic stem cells. *Nature* 448, 196–199.
- Tran, K.A., Jackson, S.A., Olufs, Z.P.G., Zaidan, N.Z., Leng, N., Kendzior, C., Roy, S., and Sridharan, R. (2015). Collaborative rewiring of the pluripotency network by chromatin and signalling modulating pathways. *Nat. Commun.* 6, 6188.
- Volarevic, V., Nurkovic, J., Arsenijevic, N., and Stojkovic, M. (2014). Concise review: therapeutic potential of mesenchymal stem cells for the treatment of acute liver failure and cirrhosis. *Stem Cells* 32, 2818–2823.
- Walton, K.M., Fisher, K., Rubitski, D., Marconi, M., Meng, Q.-J., Sládek, M., Adams, J., Bass, M., Chandrasekaran, R., Butler, T., et al. (2009). Selective inhibition of casein kinase 1 epsilon minimally alters circadian clock period. *J. Pharmacol. Exp. Ther.* 330, 430–439.
- Wei, X., Yang, X., Han, Z.-P., Qu, F.-F., Shao, L., and Shi, Y.-F. (2013). Mesenchymal stem cells: a new trend for cell therapy. *Acta Pharmacol. Sin.* 34, 747–754.
- Weinstock, J., Dunoff, R.Y., Sutton, B., Trost, B., Kirkpatrick, J., Farina, F., and Straub, A.S. (1968). Pteridines. VI. Preparation of some 6-aryl-7-aminopteridines. *J. Med. Chem.* 11, 549–556.
- Xiao, Y., and Wang, Y. (2014). Global discovery of protein kinases and other nucleotide-binding proteins by mass spectrometry. *Mass Spectrom. Rev.* <http://dx.doi.org/10.1002/mas.21447>.
- Yang, J., Van Oosten, A.L., Theunissen, T.W., Guo, G., Silva, J.C.R., and Smith, A. (2010). Stat3 activation is limiting for reprogramming to ground state pluripotency. *Cell Stem Cell* 7, 319–328.
- Yang, C.-S., Chang, K.-Y., and Rana, T.M. (2014). Genome-wide functional analysis reveals factors needed at the transition steps of induced reprogramming. *Cell Rep.* 8, 327–337.
- Yeom, Y.I., Fuhrmann, G., Ovitt, C.E., Brehm, A., Ohbo, K., Gross, M., Hubner, K., and Scholer, H.R. (1996). Germline regulatory element of Oct-4 specific for the totipotent cycle of embryonal cells. *Development* 122, 881–894.
- Zhang, J.H., Chung, T.D., and Oldenburg, K.R. (1999). A simple statistical parameter for use in evaluation and validation of high throughput screening assays. *J. Biomol. Screen.* 4, 67–73.
- Zhou, H., Li, W., Zhu, S., Joo, J.Y., Do, J.T., Xiong, W., Kim, J.B., Zhang, K., Schöler, H.R., and Ding, S. (2010). Conversion of mouse epiblast stem cells to an earlier pluripotency state by small molecules. *J. Biol. Chem.* 285, 29676–29680.
- Ziegler, S., Pries, V., Hedberg, C., and Waldmann, H. (2013). Target identification for small bioactive molecules: finding the needle in the haystack. *Angew. Chem. Int. Ed. Engl.* 52, 2744–2792.